

The impacts of $(\text{Ba,Sr})_3\text{BP}_3\text{O}_{12}:\text{Eu}^{2+}$ on the luminous flux of phosphor-converted-white light emitting diode packages

Van Liem Bui¹, Dieu An Nguyen Thi²

¹Faculty of Fundamental Science, Industrial University of Ho Chi Minh City, Ho Chi Minh City, Vietnam

²Faculty of Electrical Engineering Technology, Industrial University of Ho Chi Minh City, Ho Chi Minh City, Vietnam

Article Info

Article history:

Received Oct 30, 2021

Revised Jun 4, 2022

Accepted Jun 17, 2022

Keywords:

$(\text{Ba,Sr})_3\text{BP}_3\text{O}_{12}:\text{Eu}^{2+}$

Colour uniformity

Luminescence efficiency

Remote phosphor structure

White LED

ABSTRACT

The use of $(\text{Ba,Sr})_3\text{BP}_3\text{O}_{12}:\text{Eu}^{2+}$ in the remote phosphor structure has been proposed and analysed to offer significant improvement to the lighting performance of the phosphor-converted white light emitting diode (LED). The phosphor emits green and blue spectra centred at 520 nm and 465 nm, respectively. Thus, the phosphor can compensate the blue and green light energy components in the white-light spectral band, helping to enhance the luminous efficiency and colour uniformity of the dual-layer remote phosphor package. The increase in $(\text{Ba,Sr})_3\text{BP}_3\text{O}_{12}:\text{Eu}^{2+}$ however is not advantageous to the colour rendering index because of the lower red emission. The backscattered and back-reflected lights are degraded when the $(\text{Ba,Sr})_3\text{BP}_3\text{O}_{12}:\text{Eu}^{2+}$ phosphor layer appears in the structure. The stable chromaticity and luminous flux at good values are observed when 10% weight percentage of $(\text{Ba,Sr})_3\text{BP}_3\text{O}_{12}:\text{Eu}^{2+}$ is applied.

This is an open access article under the [CC BY-SA](https://creativecommons.org/licenses/by-sa/4.0/) license.



Corresponding Author:

Dieu An Nguyen Thi

Faculty of Electrical Engineering Technology, Industrial University of Ho Chi Minh City,

No. 12 Nguyen Van Bao Street, Ho Chi Minh City, Vietnam

Email: nguyenthidieuan@iuh.edu.vn

1. INTRODUCTION

Solid state lighting solution has been developed recently, and among the light source utilized for solid-state application, light emitting diode (LED) is the most outstanding one [1]–[3]. Owing the features of long lasting, high resistance against heat and other weather condition, excellent brightness and cost-efficiency, LEDs are considered as the most potential for future lighting devices [4]–[6]. The phosphor-converted white LED package was first fabricated with yellow phosphor and a LED die using freely dispensing technique. The procedure was simple but the lighting performance this LED fabrication method was not satisfied. The high thermal quenching and low colour rendering quality were the noticeable drawbacks resulted from this combination. To enhance the colour performance of white lights for phosphor-converted white light-emitting diodes (WLED), figuring out the efficient phosphor that can boost the red, green and blue components, under the excitation source of near-UV or blue LED dies, has been drawing tremendous attention of researchers and manufacturers. Besides, the phosphor packaging design of the LED needs to be determined to avoid the degradation in phosphor stability due to high heat generation from the LED dies. In terms of limiting the heating influence on the phosphor material, the remote phosphor can acquire high efficiency owing to the distance inserted among the phosphor film and the LED dies. Besides, it is reported that remote phosphor layer can reduce the back-scattering effects on the optical properties of LEDs [7]–[9]. However, using just one layer of yellow phosphor $\text{YAG}:\text{Ce}^{3+}$ did not successfully enrich the blue, green and red components. Therefore, using one more layer could enhance the missing colour emission to better the chromaticity and luminous flux. Hence, the selection of phosphor is crucial to the fabrication of

white LED structuring with two phosphor layers, or dual-layer remote phosphor LED package. The green phosphors that were usually studied for WLED are ZnS:Cu and SrGa₂S₄:Eu²⁺. These phosphorus sulfides could be good for the advancement of dual-layer remote phosphor structure, however presented low resistance and high degradation against humidity, which probably lowers the lifespan of the LED devices [10], [11]. The alkali borate and phosphate group have been analysed and utilized widely in laser and nonlinear lighting applications. These phosphate materials were reported to have high quantum efficacy and high thermal stability, which made them a great host matrix for synthesizing the phosphor materials having high performance on WLED applications [12], [13]. Then the borophosphate group which combines both borates and phosphates has been noticed and researched intensively in over the last decade. In terms of investigating the luminous efficiency of borophosphates, the studies focused on doping them with rare-earth ions, especially the europium ions since they are the luminescence activators that can promote great chromatic saturation and high lumen output for white LED lights [14], [15]. In this study, the Eu²⁺ ion-doped (Ba,Sr)₃BP₃O₁₂ is selected for the analysis of the optic enhancement of double-film distant phosphor LED structure. The chromaticity and luminous flux of the WLED using (Ba,Sr)₃BP₃O₁₂:Eu²⁺ phosphor layer are examined and demonstrated to provide more details on the lighting influences of different weight percentages of the green-blue emitting (Ba,Sr)₃BP₃O₁₂:Eu²⁺ phosphor.

2. METHODS

2.1. Green-blue emitting (Ba,Sr)₃BP₃O₁₂:Eu²⁺ phosphor preparation

(Ba,Sr)₃BP₃O₁₂:Eu²⁺ phosphor with green and blue emission was prepared via a solid state reaction. The ingredients include powders of BaCO₃, SrCO₃, H₃BO₃ and NH₄H₂PO₄ with the purity over 99%. After well-mixing these powders in the requisite proportions, sintering them in a furnace at 950 °C under the atmosphere of 15% H₂/85% N₂ for around 8 hours. Then, pulverizing the attained products and (Ba,Sr)₃BP₃O₁₂:Eu²⁺ phosphor is ready for further measurements. The X-ray diffractometer (Cu Kα = 1.5418 Å at 40 kV and 20 mA) was applied to provide the X-ray diffraction imaging on the crystal layout and phase purity characterizations of the preparative specimens of (Ba,Sr)₃BP₃O₁₂:Eu²⁺ phosphor. To calculate the photoluminescence of the phosphor, a spectrofluorometer of Spex Fluorolog-3, USA was utilized with two excitation monochromators and a 450 W Xeon arc lamp. Besides, the fluorescence of the phosphor samples was investigated with a photomultiplier perpendicular to the stimulation illumination. We detect the colour coordinates of the phosphor with the colour analyzer equipped with a detector (CCD) [16]. The measurements of colour rendering index and luminescence efficacy of the phosphor specimens were made at normal temperature, and attained with an EVERFINE integrating sphere. It was observed that the phosphor (Ba,Sr)₃BP₃O₁₂:Eu²⁺ showed a broad excitation band (300-400 nm) matching the excitation wavelength of the near-UV LED dies. As a results, the bright green and bluish-white emission could be generated, depending on the doped concentration of the ion Eu²⁺. According to Blasse's study on the energy transfer of the activator which is presented only on Z ion points, the crucial transfer distance R_c can be expressed as [17]–[19]:

$$R_c \approx 2 \left(\frac{3V}{4\pi x_c N} \right)^{1/3} \quad (1)$$

in which, x_c shows the crucial concentration, N indicates the Z ion numbers in the unit cell, and V presents the volume unite cell. It is noted that there is one activator ion per $\frac{V}{x_c N}$ volume, and the R_c is relatively double the radius of a sphere with this volume. Regarding to the luminescence intensity of the phosphor sample, the emission intensity on per activator concentration is calculated by (2).

$$\frac{I}{x} = \frac{k}{1+\beta(x)^{\theta/3}} \quad (2)$$

Here, I and x are the emission intensity and the concentration of ion activator, respectively. θ is respectively 6, 8, 10 for the interactions of dipole-dipole, dipole-quadrupole, quadrupole-quadrupole, while k and β are constant for each interaction. Obviously, on a log scale, the parameter I/x depends greatly on x , which was slightly linear. Additionally, the slope ($-\theta/3$) was detected at about -1.92. Consequently, θ can be computed to be 5.76, relatively equal to 6, indicating that the mechanism of Eu²⁺-ion concentration quenching was controlled by the dipole-dipole interaction [10], [20]. The replacement of Sr²⁺ cation to Ba²⁺ one was responsible for the strength enhancement of the crystal field, in connection with the reduction in bond length, whose relation can be demonstrated as [21], [22].

$$D_q = 3Ze^2r^4/5R^5 \quad (3)$$

D_q shows the strength of crystal region, R indicates the centre ion-ligands bond lengthiness. According to this, the enhanced crystal field strength could lead to the red shift for Eu^{2+} ion state transition of $5d \rightarrow 4f$. Besides, the blue shift in the emission of the phosphor can be demonstrated by the decreasing nephelauxetic effect of the $\text{Eu}-\text{O}$ bonds occurring when the smaller Sr^{2+} alternates the Ba^{2+} cations [23], [24].

2.2. The simulation of double-film distant phosphor WLED structure

Applying the lighting engineering software of LightTools version 9.0 and Monte Carlo method is essential to give highly accurate measurements, which helps to effectively simulate the WLED models for investigating the optical influences of $(\text{Ba,Sr})_3\text{BP}_3\text{O}_{12}:\text{Eu}^{2+}$ phosphor with tuneable colour emission of green and blue. The phosphor films are modeled with flat silicone layer. After designing the simulated WLED packages with the colour heats of 5,600 K and 8,500 K, the concentration of green-blue phosphor $(\text{Ba,Sr})_3\text{BP}_3\text{O}_{12}:\text{Eu}^{2+}$ is adjusted in the range of 5-15 wt%. Depending on the added concentration of green-blue phosphor, the optical properties of the phosphor packages, including the efficiency in light scattering, absorption, transmission, and extraction, all of which greatly impact the chromaticity and luminescence performance of the generated white light of a LED. This can be also ascribed to the change in yellow-color phosphor $\text{YAG}:\text{Ce}^{3+}$ concentration respectively to the increase of $(\text{Ba,Sr})_3\text{BP}_3\text{O}_{12}:\text{Eu}^{2+}$ percentage in the structure. The applied remote phosphor design is the dual-layer one because of its higher light efficiency, compared to the single-film remote phosphor package. Each phosphor layer is 0.08 mm thick and put above the nine blue LED chips. The set of nine LED chip are demonstrated in three parallel columns an embedded to the reflector cavity, as shown in Figure 1. The size parameters of a chip are 1.14 mm² and 0.15 mm in its square base surface and height, respectively. In addition, each of them performs the illuminating power of 1.16 W with the maximum wavelength of 453 nm. Besides, the measurements of the reflector in surface and bottom lengths and height are 9.85×8×2.07 mm.

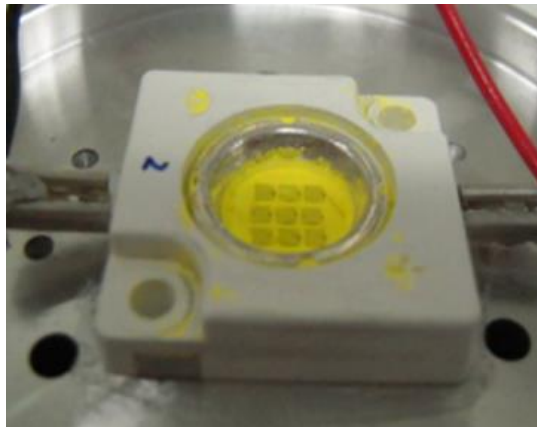


Figure 1. Picture of WLEDs

3. RESULTS AND DISCUSSION

When heightening the percentage of $(\text{Ba,Sr})_3\text{BP}_3\text{O}_{12}:\text{Eu}^{2+}$ phosphor in the LED structure, the lowered concentration of $\text{YAG}:\text{Ce}^{3+}$ was observed. As illustrated in Figure 2, the concentration of $\text{YAG}:\text{Ce}^{3+}$ phosphor decreased when higher $(\text{Ba,Sr})_3\text{BP}_3\text{O}_{12}:\text{Eu}^{2+}$ was presented. The reduction in yellow phosphor concentration could benefits the light output of the LED package by keeping the colour temperature at stable values (5,600 K and 8,500 K) and reducing the back-scattered and back-reflected lights, see Figure 2(a). Besides, high concentration of yellow $\text{YAG}:\text{Ce}^{3+}$ was reported as one of the main causes of higher thermal generation of the phosphor layer, leading to the degradation in phosphor conversion efficiency, as shown in Figure 2(b). Since the yellow phosphor absorbed and converted a part blue lights from LED chips into yellow lights, high concentration of yellow phosphor $\text{YAG}:\text{Ce}^{3+}$ probably decrease the colour rendering index (CRI) of the LED due to the yellow light dominating the blue light proportions. Therefore, maintaining lower yellow phosphor layer concentration could result in higher white-light quality of a phosphor-converted WLED. Hence, $(\text{Ba,Sr})_3\text{BP}_3\text{O}_{12}:\text{Eu}^{2+}$ can be a promising material for further development of the remote phosphor-converted WLED models.

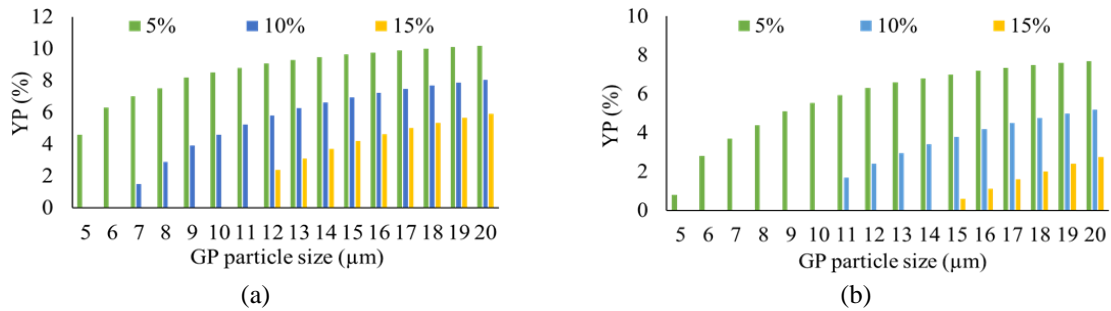


Figure 2. The variation in phosphor concentration for the mean of the stable CCT: (a) 5,600 K and (b) 8,500 K

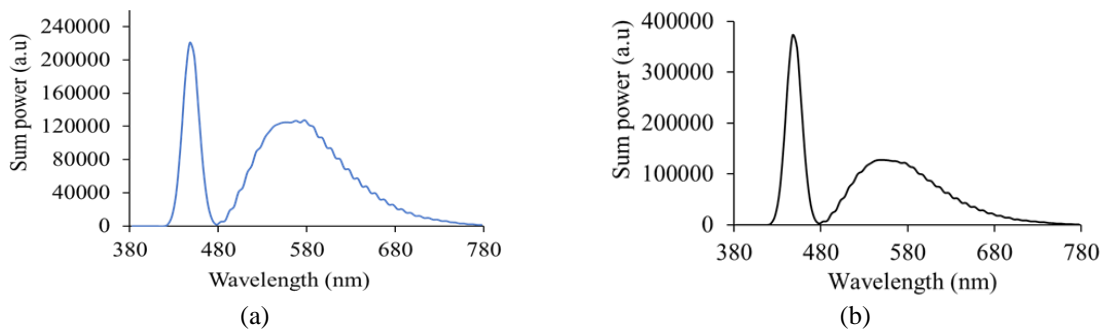


Figure 3. The emitting spectra of WLEDs as a function of $(\text{Ba,Sr})_3\text{BP}_3\text{O}_{12}:\text{Eu}^{2+}$ concentration: (a) 5,600 K and (b) 8,500 K

The phosphor $(\text{Ba,Sr})_3\text{BP}_3\text{O}_{12}:\text{Eu}^{2+}$, when being applied to the dual-remote phosphor WLED package, considerably affected the spectral emission energy of the emitted white lights, see Figure 3. Figure 3(a) clearly displayed this influence on the WLED with two CCTs of 5,600 K and 8,500 K. In particular, the addition of $(\text{Ba,Sr})_3\text{BP}_3\text{O}_{12}:\text{Eu}^{2+}$ phosphor enhance the emission intensities at the blue and green wavelengths, see Figure 3(b). This implies that there are more blue and green lights generated and the combined with the converted yellow lights to form white lights with a more uniform colour distribution. Moreover, the blue-green spectral energy enhancement can be also attributed to the decline in yellow phosphor $\text{YAG}:\text{Ce}^{3+}$ concentration, which offer the minimization to the backscattering effects to enhance the blue-light transmission. Meanwhile, the green light components are supplemented by the excited green emission region of the phosphor $(\text{Ba,Sr})_3\text{BP}_3\text{O}_{12}:\text{Eu}^{2+}$. In addition to that, this also implies the enhancement scattering ability of blue lights, contributing to growing the uniformity of angular white-light chromaticity. Plus, the upward trend in lighting performances of the dual-layer remote WLED is observed at both 5,600 K and 8,500 K correlated colour temperature, which indicates the possibility of using green-blue $(\text{Ba,Sr})_3\text{BP}_3\text{O}_{12}:\text{Eu}^{2+}$ phosphor to accomplish the desired high homogeneity in chromatic property of remote phosphor packages operating at high CCTs.

The lumen efficiency of WLED with $(\text{Ba,Sr})_3\text{BP}_3\text{O}_{12}:\text{Eu}^{2+}$ phosphor was further demonstrated in Figure 4. The more the weight percentage of the green phosphor increases, the higher the luminous intensity of the WLED can be obtained. When the concentration of the green-blue emitting phosphor was added up to 15% wt., the luminous output of the dual-layer LED models reached the highest values, regardless of the green phosphor particle sizes and correlated colour temperatures, see Figure 4(a). Ascribing to the absorption characteristic of $(\text{Ba,Sr})_3\text{BP}_3\text{O}_{12}:\text{Eu}^{2+}$ phosphor, the blue light and yellow illumination released from the LED chip and $\text{YAG}:\text{Ce}^{3+}$ phosphor layer are absorbed when reaching this green-blue phosphor layer. Then, these absorbed light by $(\text{Ba,Sr})_3\text{BP}_3\text{O}_{12}:\text{Eu}^{2+}$ are converted to enrich blue and green peaks, leading to the balanced chromatic energy distribution in the spectral emission of the LED white lights, as shown in Figure 4(b). Therefore, the dual-layer remote LED package can achieve minimal colour-deviation values, or higher colour homogeneity, as shown in Figure 5. Both Figure 5(a) and Figure 5(b) presented the improvement in colour deviation features of the dual-layer structure in accordance with the increase of $(\text{Ba,Sr})_3\text{BP}_3\text{O}_{12}:\text{Eu}^{2+}$ phosphor concentration, which reinforces the benefits of using this phosphor to promote better optical performances of remote-phosphor WLEDs.

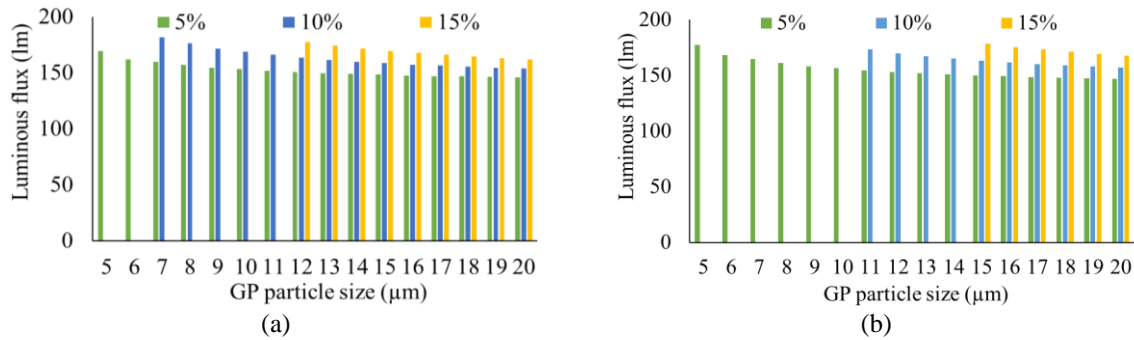


Figure 4. The illuminating beam of WLEDs as a function of $(\text{Ba,Sr})_3\text{BP}_3\text{O}_{12}:\text{Eu}^{2+}$ concentration: (a) 5,600 K and (b) 8,500 K

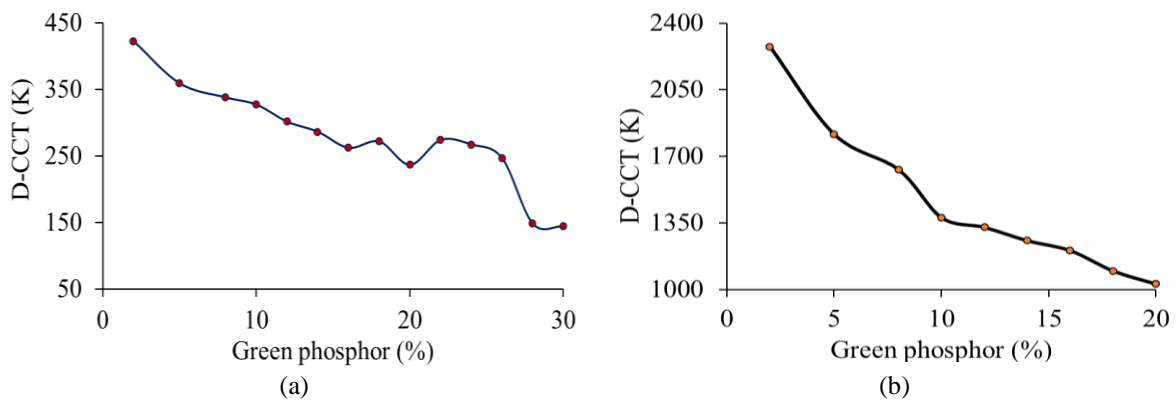


Figure 5. The color deviation of WLEDs as a function of $(\text{Ba,Sr})_3\text{BP}_3\text{O}_{12}:\text{Eu}^{2+}$ concentration: (a) 5,600 K and (b) 8,500 K

In the lighting market, the color rendering index (CRI) is regarded as among the most critical decision variables whether the a light source’s hue faithfulness is high. The CRI test compares the color of an object revealed under an experimented light source with that of the reference one, usually the blackbody radiation. The higher the CRI that the light source gets, the higher the color accuracy becomes. Here, the increase of $(\text{Ba,Sr})_3\text{BP}_3\text{O}_{12}:\text{Eu}^{2+}$ concentration is not advantageous to the CRI since there is a lack of red emission while the blue and green emissions increase, see Figure 6. As can be seen in Figure 6(a), the CRI of the WLEDs models was below 60 when the concentration of green phosphor $(\text{Ba,Sr})_3\text{BP}_3\text{O}_{12}:\text{Eu}^{2+}$ reached 15% wt. Thus, if the goal is to achieve high CRI, the concentration of this phosphor should be remained below 10% wt, see Figure 6(b). However, CRI is not the most optimal color assessment parameter because of its limited color samples (around 8 samples) for testing. Though high CRI is often accompanied with higher prices of LED devices in the market, it cannot assure that the color quality of this LED is superb. Therefore, the other color evaluating index has been taken into consideration, which is the color quality scale proposed by NIST research team. Their report demonstrated that, colour quality scale is a parameter that accesses the chromatic evaluation via three elements of CRI, colour coordinates and the visual preference of observers. Thus, acquiring high CQS is more challenging than attaining high CRI [25]. The increase of $(\text{Ba,Sr})_3\text{BP}_3\text{O}_{12}:\text{Eu}^{2+}$ concentration to 10% wt. can elevated the color quality scale of the dual-layer WLED structure, as can be observed in Figure 7. Specifically, in the structure with 5,600 K CCT, the rise in $(\text{Ba,Sr})_3\text{BP}_3\text{O}_{12}:\text{Eu}^{2+}$ concentration is not completely favoured by the CQS since the highest the CQS values were obtained at 5% wt, and gradually reduced with higher concentration of this green phosphor. On the other hand, at higher CCT of 8500 K, the growth in phosphor concentration of $(\text{Ba,Sr})_3\text{BP}_3\text{O}_{12}:\text{Eu}^{2+}$ layer did have positive effects on the CQS of the package, see Figure 7(a). When there was 10% wt. of $(\text{Ba,Sr})_3\text{BP}_3\text{O}_{12}:\text{Eu}^{2+}$, the CQS was slightly enhance and stable at around more than 62. Thus, it is possible to achieve better colour rendering and uniformity of the WLED with dual-layer remote phosphor design by using 10% $(\text{Ba,Sr})_3\text{BP}_3\text{O}_{12}:\text{Eu}^{2+}$, an vital information for manufacturers to consider in their production procedure, see Figure 7(b).

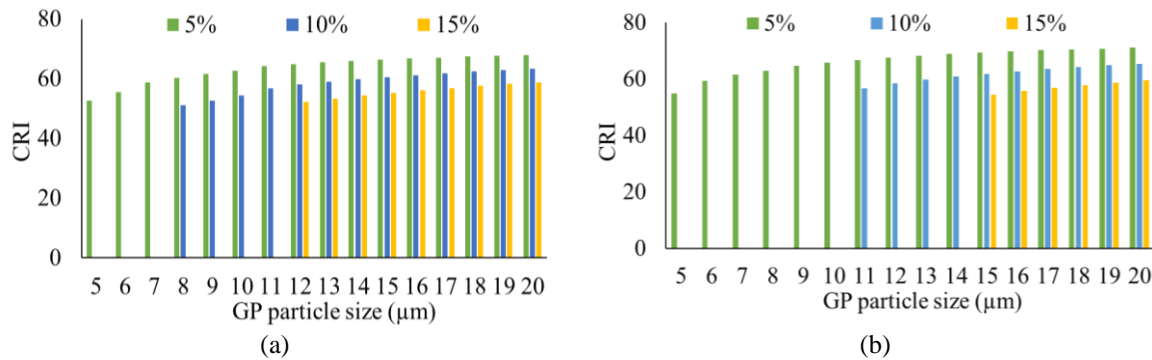


Figure 6. The color rendering index of WLEDs as a function of $(\text{Ba,Sr})_3\text{BP}_3\text{O}_{12}:\text{Eu}^{2+}$ concentration: (a) 5,600 K and (b) 8,500 K

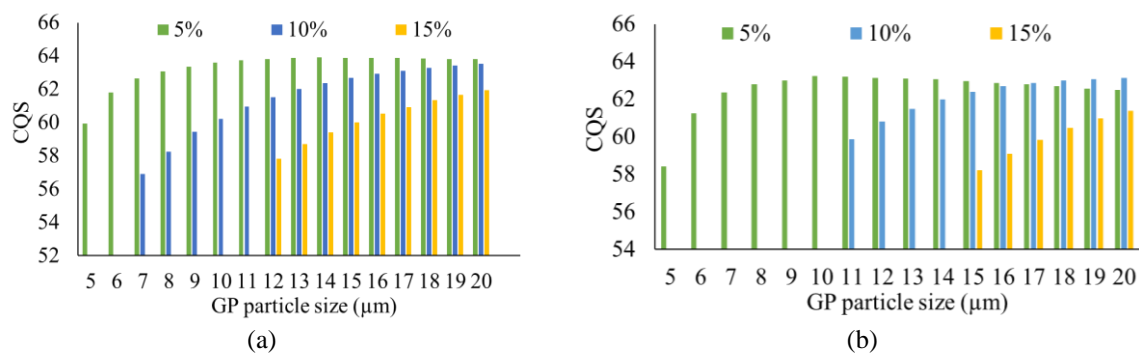


Figure 7. The color quality scale of WLEDs as a function of $(\text{Ba,Sr})_3\text{BP}_3\text{O}_{12}:\text{Eu}^{2+}$ concentration: (a) 5,600 K and (b) 8,500 K

4. CONCLUSION

The effective phosphor offering green and blue emission, $(\text{Ba,Sr})_3\text{BP}_3\text{O}_{12}:\text{Eu}^{2+}$ was prepared, characterized and analysed in this study. The impacts of this structure on the optical properties of chromaticity and illumination strength of the WLED with double-film distant phosphor package at 5600 K and 8500 K are the main topic. After conducting experiments and measurements, this green-blue emitting phosphor can be the potential for advanced WLED production in the future. The colour parameters, CQS and colour variances, of the LED is improved with the presence of $(\text{Ba,Sr})_3\text{BP}_3\text{O}_{12}:\text{Eu}^{2+}$ phosphor, specifically used at 10% wt. On the other hand, the high concentration of $(\text{Ba,Sr})_3\text{BP}_3\text{O}_{12}:\text{Eu}^{2+}$ relatively has negative effects on the CRI since the red emission peak is shortage while the blue and green lights components are enhanced. This case leads to colour imbalance and light loss in the LED model. Besides, the increase of $(\text{Ba,Sr})_3\text{BP}_3\text{O}_{12}:\text{Eu}^{2+}$ amount is noticeably.




REFERENCES

- [1] R. Guerreiro, I. Carpinteiro, L. Proença, M. Polido, and A. Azul, "Influence of acid etching on internal bleaching with 16% carbamide peroxide," *Ann. Med.*, vol. 53, no. sup1, pp. S48–S49, Apr. 2021, doi: 10.1080/07853890.2021.1897351.
- [2] A. Vagge, L. Ferro Desideri, C. Del Noce, I. Di Mola, D. Sindaco, and C. E. Traverso, "Blue light filtering ophthalmic lenses: A systematic review," *Semin. Ophthalmol.*, vol. 36, no. 7, pp. 541–548, Oct. 2021, doi: 10.1080/08820538.2021.1900283.
- [3] S. Kadyan, S. Singh, S. Sheoran, A. Samantilleke, B. Mari, and D. Singh, "Synthesis and optoelectronic characteristics of $\text{MGdAl}_3\text{O}_7:\text{Eu}^{3+}$ nanophosphors for current display devices," *Trans. Indian Ceram. Soc.*, pp. 219–226, Dec. 2019, doi: 10.1080/0371750X.2019.1690583.
- [4] S. Sheoran *et al.*, "Synthesis and optoelectronic characterization of silicate lattice-based $\text{M}_3\text{La}_2\text{Si}_3\text{O}_{12}$ ($\text{M} = \text{Mg}^{2+}$, Ca^{2+} , Sr^{2+} and Ba^{2+}) nanophosphors for display applications," *Trans. Indian Ceram. Soc.*, vol. 79, no. 1, pp. 35–42, Jan. 2020, doi: 10.1080/0371750X.2020.1712259.
- [5] E. Bowditch, E. Chu, T. Hong, and A. A. Chang, "Treat and extend paradigm in management of neovascular age-related macular degeneration: current practice and future directions," *Expert Rev. Ophthalmol.*, vol. 16, no. 4, pp. 267–286, Jul. 2021, doi: 10.1080/17469899.2021.1933439.
- [6] J. S. Pozo-Antonio and P. Sanmartín, "Exposure to artificial daylight or UV irradiation (A, B or C) prior to chemical cleaning: an effective combination for removing phototrophs from granite," *Biofouling*, vol. 34, no. 8, pp. 851–869, Sep. 2018, doi: 10.1080/08927014.2018.1512103.




- [7] L. M. Negi, S. Talegaonkar, M. Jaggi, and A. K. Verma, "Hyaluronated imatinib liposomes with hybrid approach to target CD44 and P-gp overexpressing MDR cancer: an in-vitro, in-vivo and mechanistic investigation," *J. Drug Target.*, vol. 27, no. 2, pp. 183–192, Feb. 2019, doi: 10.1080/1061186X.2018.1497039.
- [8] M. Alavi and M. Rai, "Recent advances in antibacterial applications of metal nanoparticles (MNPs) and metal nanocomposites (MNCs) against multidrug-resistant (MDR) bacteria," *Expert Rev. Anti. Infect. Ther.*, vol. 17, no. 6, pp. 419–428, Jun. 2019, doi: 10.1080/14787210.2019.1614914.
- [9] A. C. F. Vendette, H. L. Piva, L. A. Muehlmann, D. A. de Souza, A. C. Tedesco, and R. B. Azevedo, "Clinical treatment of intra-epithelia cervical neoplasia with photodynamic therapy," *Int. J. Hyperth.*, vol. 37, no. 3, pp. 50–58, Dec. 2020, doi: 10.1080/02656736.2020.1804077.
- [10] M. Talone and G. Zibordi, "Spatial uniformity of the spectral radiance by white LED-based flat-fields," *OSA Contin.*, vol. 3, no. 9, p. 2501, Sep. 2020, doi: 10.1364/OSAC.394805.
- [11] V. Bahrami-Yekta and T. Tiedje, "Limiting efficiency of indoor silicon photovoltaic devices," *Opt. Express*, vol. 26, no. 22, p. 28238, Oct. 2018, doi: 10.1364/OE.26.028238.
- [12] B. Li *et al.*, "High-efficiency cubic-phased blue-emitting Ba₃Lu₂B₆O₁₅:Ce³⁺ phosphors for ultraviolet-excited white-light-emitting diodes," *Opt. Lett.*, vol. 43, no. 20, p. 5138, Oct. 2018, doi: 10.1364/OL.43.005138.
- [13] S. Cincotta, C. He, A. Neild, and J. Armstrong, "High angular resolution visible light positioning using a quadrant photodiode angular diversity aperture receiver (QADA)," *Opt. Express*, vol. 26, no. 7, p. 9230, Apr. 2018, doi: 10.1364/OE.26.009230.
- [14] Q. Hu, X. Jin, and Z. Xu, "Compensation of sampling frequency offset with digital interpolation for OFDM-based visible light communication systems," *J. Light. Technol.*, vol. 36, no. 23, pp. 5488–5497, Dec. 2018, doi: 10.1109/JLT.2018.2876042.
- [15] A. I. Alhassan *et al.*, "Development of high performance green c-plane III-nitride light-emitting diodes," *Opt. Express*, vol. 26, no. 5, p. 5591, Mar. 2018, doi: 10.1364/OE.26.005591.
- [16] J. Cheng *et al.*, "Luminescence and energy transfer properties of color-tunable Sr₄La(PO₄)₃O:Ce³⁺, Tb³⁺, Mn²⁺ phosphors for WLEDs," *Opt. Mater. Express*, vol. 8, no. 7, p. 1850, Jul. 2018, doi: 10.1364/OME.8.001850.
- [17] J.-S. Li, Y. Tang, Z.-T. Li, L.-S. Rao, X.-R. Ding, and B.-H. Yu, "High efficiency solid-liquid hybrid-state quantum dot light-emitting diodes," *Photonics Res.*, vol. 6, no. 12, p. 1107, Dec. 2018, doi: 10.1364/PRJ.6.001107.
- [18] Y. Peng *et al.*, "Flexible fabrication of a patterned red phosphor layer on a YAG:Ce³⁺ phosphor-in-glass for high-power WLEDs," *Opt. Mater. Express*, vol. 8, no. 3, p. 605, Mar. 2018, doi: 10.1364/OME.8.000605.
- [19] K. Werfli *et al.*, "Experimental demonstration of high-speed 4 × 4 imaging multi-CAP MIMO visible light communications," *J. Light. Technol.*, vol. 36, no. 10, pp. 1944–1951, May 2018, doi: 10.1109/JLT.2018.2796503.
- [20] W. Zhong, J. Liu, D. Hua, S. Guo, K. Yan, and C. Zhang, "White LED light source radar system for multi-wavelength remote sensing measurement of atmospheric aerosols," *Appl. Opt.*, vol. 58, no. 31, p. 8542, Nov. 2019, doi: 10.1364/AO.58.008542.
- [21] S. Feng and J. Wu, "Color lensless in-line holographic microscope with sunlight illumination for weakly-scattered amplitude objects," *OSA Contin.*, vol. 2, no. 1, p. 9, Jan. 2019, doi: 10.1364/OSAC.2.000009.
- [22] J.-O. Kim, H.-S. Jo, and U.-C. Ryu, "Improving CRI and scotopic-to-photopic ratio simultaneously by spectral combinations of CCT-tunable LED lighting composed of multi-chip LEDs," *Curr. Opt. Photonics*, vol. 4, no. 3, pp. 247–252, 2020.
- [23] X. Ding *et al.*, "Improving the optical performance of multi-chip LEDs by using patterned phosphor configurations," *Opt. Express*, vol. 26, no. 6, p. A283, Mar. 2018, doi: 10.1364/OE.26.00A283.
- [24] Z. Zhao, H. Zhang, S. Liu, and X. Wang, "Effective freeform TIR lens designed for LEDs with high angular color uniformity," *Appl. Opt.*, vol. 57, no. 15, p. 4216, May 2018, doi: 10.1364/AO.57.004216.
- [25] C. Jaques, E. Pignat, S. Calinon, and M. Liebling, "Temporal super-resolution microscopy using a hue-encoded shutter," *Biomed. Opt. Express*, vol. 10, no. 9, pp. 4727–4741, Aug. 2019, doi: 10.1364/BOE.10.004727.

BIOGRAPHIES OF AUTHORS



Van Liem Bui    received a Bachelor of Mathematical Analysis and master's in mathematical Optimization, Ho Chi Minh City University of Natural Sciences, VietNam. Currently, He is a lecturer at the Faculty of Fundamental Science, Industrial University of Ho Chi Minh City, Viet Nam. His research interests are mathematical physics. He can be contacted at email: buivanliem@iuh.edu.vn.



Dieu An Nguyen Thi    received a master of Electrical Engineering, HCMC University of Technology and Education, VietNam. Currently, she is a lecturer at the Faculty of Electrical Engineering Technology, Industrial University of Ho Chi Minh City, Viet Nam. Her research interests are theoretical physics and mathematical physics. She can be contacted at email: nguyenthidieuan@iuh.edu.vn.